Wind and Structures, Vol. 11, No. 2 (2008) 137-152
DOI: http://dx.doi.org/10.12989/was.2008.11.2.137

A forensic study of the Lubbock-Reese downdraft of 2002

J. D. Holmes[1,2] and H. M. Hangan*[2]

[1]JDH Consulting, Mentone, Victoria, 3194 Australia
[2]University of Western Ontario, London, Ontario N6A 5B9, Canada

J. L. Schroeder

Texas Tech University, Lubbock, Texas, USA

C. W. Letchford

University of Tasmania, Private Bag 65, Hobart, Tasmania, 7001, Australia

K. D. Orwig

Texas Tech University, Lubbock, Texas, USA
(Received October 18, 2007, Accepted March 5, 2008)

Abstract. This paper discusses engineering aspects of the rear-flank downdraft that was recorded near Lubbock, Texas on 4 June 2002, and produced a gust wind speed nearly equal to the design value (50-year return period) for the region. The general characteristics of the storm, and the decomposition of the time histories into deterministic 'running mean' and random turbulence components are discussed. The fluctuating wind speeds generated by the event can be represented as a dominant low-frequency 'running-mean', with superimposed random turbulence of higher frequencies. Spectral and correlation characteristics of the residual turbulence are found to be similar to those of high-frequency turbulence in boundary-layer winds. However, the low-frequency components in the running-mean wind speeds are spatially homogeneous, in contrast to the low-frequency turbulence found in synoptic boundary-layer winds. With respect to transmission line design, this results in significantly higher 'span reduction factors'.

Keywords: downdraft; rear-flank; supercell; thunderstorm; turbulence; transmission-line.

1. Introduction

Convective downdraft winds, usually associated with thunderstorms, are known to produce damaging winds near ground level, with magnitudes of wind speed of relevance to structural design. In the equatorial latitudes of the world, and in many inland continental regions between 10 and about 40 degrees latitude, these events appear to be the dominant storm type for structural design of

* Associate Professor and Director, Corresponding Author, E-mail: hmh@blwtl.uwo.ca

low and medium height structures. Amongst others, Holmes (1999) and Letchford, *et al.* (2002) have reviewed the significance of thunderstorm winds, in particular severe convective downdrafts, and their importance for wind loads on structures.

However, the characteristics of these storm types – vertical and horizontal velocity profiles, turbulence characteristics etc., have not yet generally been adopted for structural design – either for wind-tunnel tests, or by design codes and standards, which are normally based on the characteristics of large-scale synoptic boundary-layer winds, even in locations where thunderstorm downdrafts are the dominant extreme wind type. One reason for this has been the lack of reliable, and sufficiently detailed, full-scale measurements, for events with high enough wind speed. However, the rear-flank downdraft (RFD) recorded at Lubbock, Texas, in 2002, (Gast-Orwig and Schroeder 2003, Orwig and Schroeder 2007) has recently provided a unique data record for events of this type. Another reason is that there are clearly several different types and scales of convective downdrafts (Wakimoto 2001), the smaller microburst has generally received more attention up to now.

In this paper, a forensic analysis of the Reese-Lubbock rear-flank downdraft, with emphasis on engineering design applications is described. The characteristics of the storm, and a methodology for decomposing the wind speed time histories, are discussed. In later sections, analyses of the deterministic and random components are described.

2. General characteristics

The Wind Science and Engineering Research Center at Texas Tech University was very fortunate to be able to record the gust front from a severe downdraft that occurred during the evening of June 4, 2002, at the former Reese Air Force base, about 20 km west of the centre of Lubbock, Texas, with an array of anemometers. The line of anemometer towers ran approximately north-south with a spacing of 263 m between adjacent towers. Propeller-vane anemometers were used; the anemometers were located at 10 metres height on Towers 2, 3, 4 and 5. Tower 4 also had anemometers at 2, 4, 6 and 15 metres. More details of the measurement system and the basic anemometer records were given by Gast-Orwig and Schroeder (2003, 2007).

A maximum wind gust of slightly greater than 40 m/s was recorded on the anemometer on Tower 3 - coincidentally the 50-year return-period wind speed for the area, used in the American Loading Standard ASCE-7 (ASCE 2005). The event was associated with the rear flank of a 'supercell' thunderstorm as revealed by the Doppler WSR-88D weather radar at the Lubbock Airport (Fig. 1). The elevation angle of the radar sweep shown in Fig. 1 was 1.54 degrees, meaning that the height of the reflectivity image was about 500 metres above ground level at a distance of 20 kilometres from the radar. The image of the downdraft thus shows reflections from water droplets at approximately this height.

The event produced peak gusts that occurred nearly simultaneously along the array of seven towers at the Reese site. Animation of the radar images show a large curved radar echo – travelling from west to east, and traversing the anemometer tower array nearly normal to the north-south line. The times of the radar echo crossing the towers at both Reese and Lubbock Airport corresponded closely with the times at which maximum wind speeds were recorded (see later discussion).

Various types of severe convective downdrafts that have been identified as producing strong winds are discussed by Wakimoto (2001). It should be noted that the rear-flank downdraft is identified as a different type of event to the 'microburst', as the Andrews AFB event of 1983 was classified (Fujita 1985).

The wind speed and direction recorded by the anemometer at 10 metres height on Tower No. 4 at

Reese near the centre of the north-south array is shown in Fig. 2. Data was sampled at 1-second intervals.

Before the main gust front arrived, the wind speed was around 15 m/s from the east, probably resulting from the mesoscale pressure gradient left from earlier convective activity. As the gust front passed over the anemometer, a 180 degree wind direction change, at about 270 seconds, coincided with the rapid build up in wind speed from below 5 m/s to above 35 m/s at about 500 seconds from the start of the record. At about 700 seconds the wind direction shifted back through 180 degrees – i.e. from the east, and the wind speed dropped to about 10 m/s. In this record, the maximum wind speed of 39 m/s presumably comprises a component due to the forward motion of the gust front and one due to velocities within the frontal structure – assumed to be a large ring vortex. The wind field following the second change in direction (at about 700 sec) may be related to the passage of ring vortices moving in an easterly direction relative to the centre-line, see Kim and Hangan (2007).

Fig. 3 shows the individual time histories from 10 metres height from Towers 3, 4, 5 and 6; each tower was separated from its neighbour by a distance of 263 m. The general similarity of the underlying slow period fluctuations in wind speed at the various towers, are shown in Fig. 3. This aspect, and the

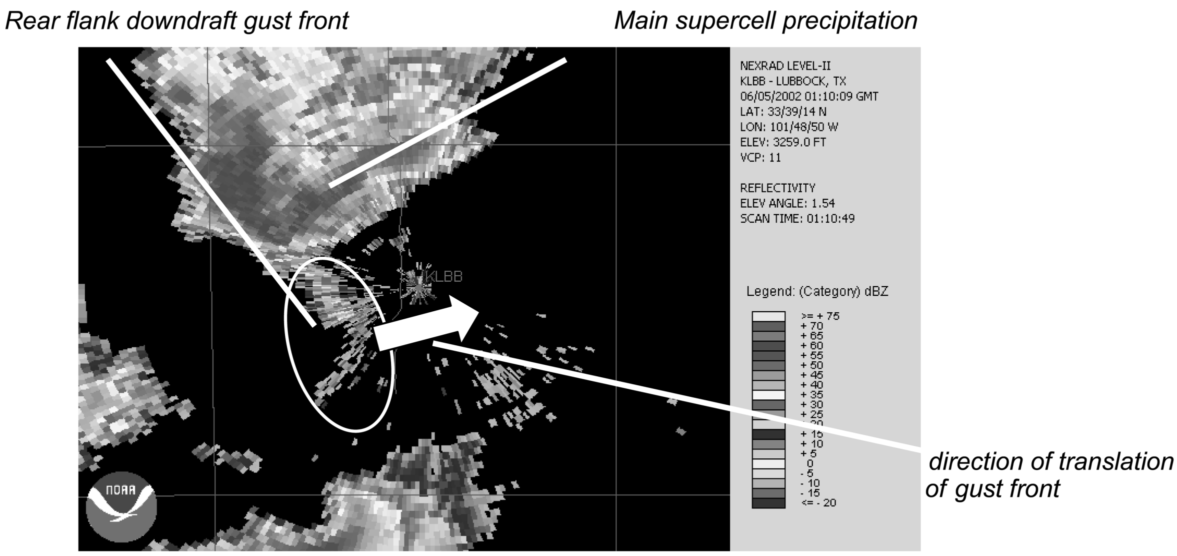

Fig. 1 Radar image, at 19:10 Central Standard Time, showing a super-cell thunderstorm and associated rear-flank gust front west of Lubbock

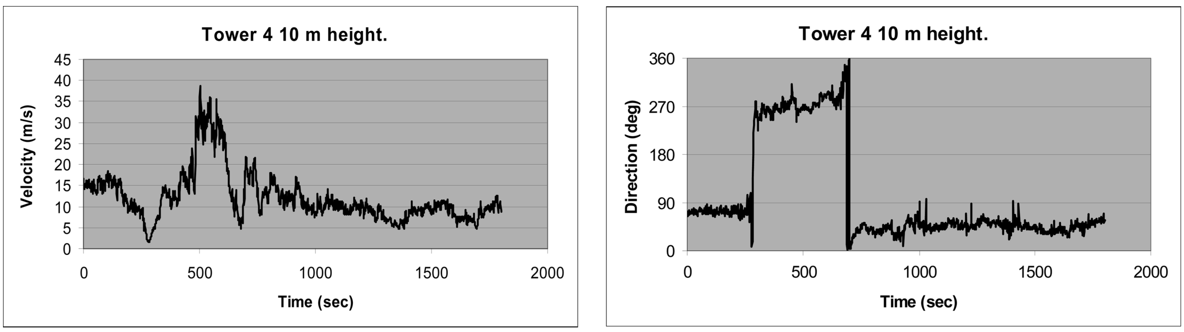

Fig. 2 Wind speed and direction at Reese (10 metres height on Tower 4)

significance for systems of horizontal extent, like transmission lines, is discussed later in the paper.

The maximum 5-second gusts in every minute were also available from ASOS data recorded at Lubbock Airport, about 22 kilometres ENE of Reese (its location is close to the radar station, at the centre of the image on Fig. 1). These data, together with the wind direction every minute, for the period between 18:00 and 21:00 Central Standard Time (CST) on 4th June, are shown in Fig. 4 (on the wind direction plot some values have had 360 degrees subtracted to improve the appearance of the graph). There is a 180-degree wind shift that lasts for about 8 minutes (a similar time period to the Reese data in Fig. 2), and a peak wind gust of 21 m/s at about 19:23 CST. This time is almost exactly 30 minutes after the event recorded at Reese. The similarity of the wind direction shift indicates that it is the same event, although the wind speed is considerably weaker. The radar data

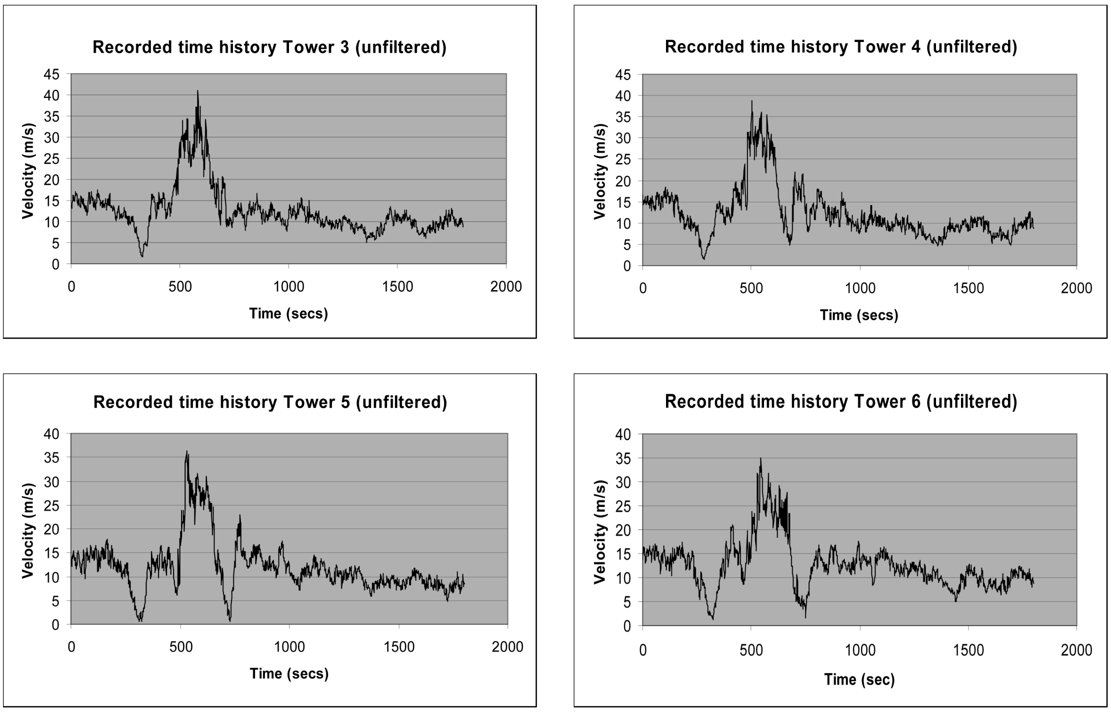

Fig. 3 Wind speed from four towers at Reese (10 metres height)

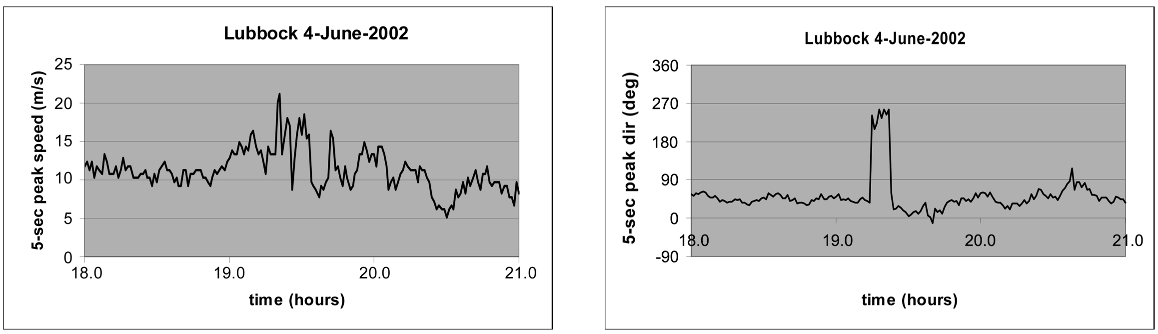

Fig. 4 Wind speed and direction from 1-minute ASOS data from Lubbock Airport

confirms this, and the weaker wind speeds are due to the on-going dissipation of the storm during the aforementioned 30 minute time period.

The time delay indicates a gust front speed of about 44 km/hour, or 12 m/s. This value agrees with translation speed of the radar echoes recorded by the WSR-88D radar at Lubbock Airport.

3. Decomposition of wind speed-time histories

It is logical to decompose the individual anemometer records from the Reese site into a slowly-varying deterministic 'running-mean', and residual random 'turbulence' components. This method was proposed for thunderstorm wind data by Choi and Hidayat (2002), and corresponds to the well-established decomposition of a turbulence signal into a phase average (mean plus coherent parts) and a random component, (Jeong and Hussain 1995). However, Chen and Letchford (2005, 2006) have used (different) decomposition approaches to the Reese data set.

A simple engineering method of filtering the original time histories for the running-mean is to use a moving average filter. Such filtering was carried out for a number of different moving average times, and Fig. 5 shows the effect of a moving average, with averaging times of 10, 40 and 60 seconds, on the wind speed- time histories from Tower 4 (10 m height).

The following criteria were used to select an appropriate averaging time to filter the wind speed records:

- The main features of the flow represented by the main low-frequency peaks and troughs, should be retained, and
- the residual turbulence that remains after subtracting the filtered time history from the original record should have a near-zero mean value.

The first criterion relates to the preservation of the signatures related to the significant flow

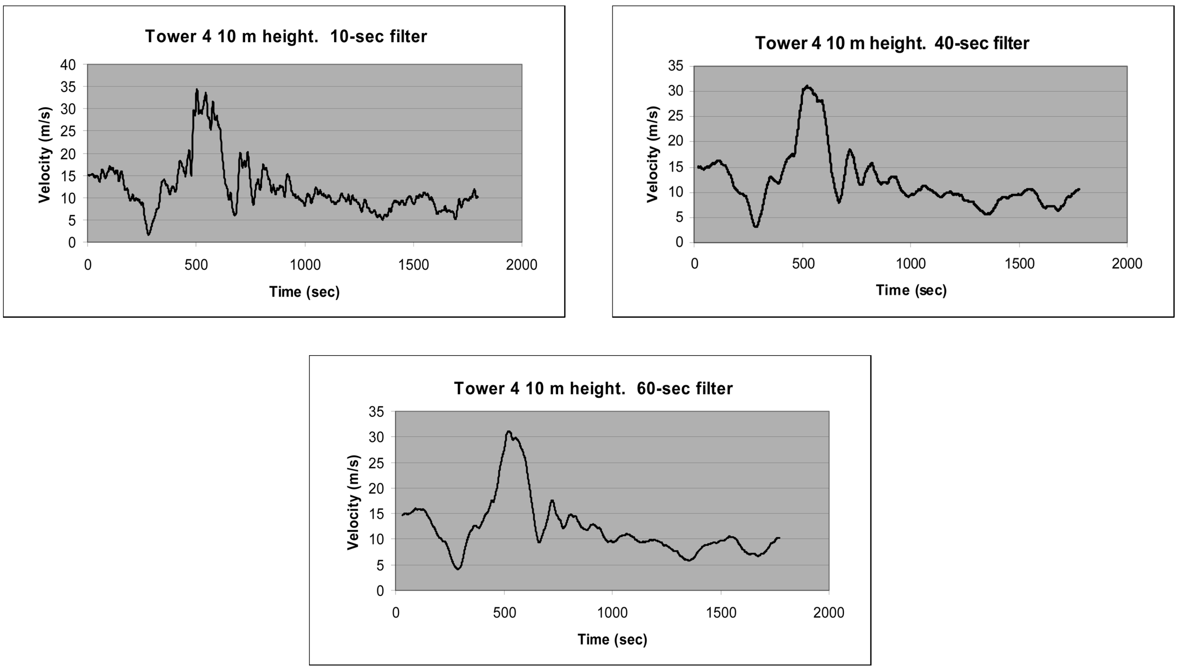

Fig. 5 Effect of averaging time on wind speed time history

features, including the main vortices and is somewhat subjective. However, the second criterion can be checked by calculating the mean values of the residual time histories- i.e., the sample means of the random turbulence. This has been done and the results are shown in Fig. 6. This shows that near-zero mean values occur for averaging times less than about 100 seconds. For averaging times greater than this value clearly some significant low-frequency components reflecting the main flow features are retained. This is a significant difference between thunderstorm time histories and those of large scale synoptic events (i.e. temperate gales or tropical cyclones), and processing and engineering design criteria should be adjusted accordingly. An obvious conclusion is that codification based on 10-minute or hourly means is not appropriate for locations where thunderstorm downdrafts

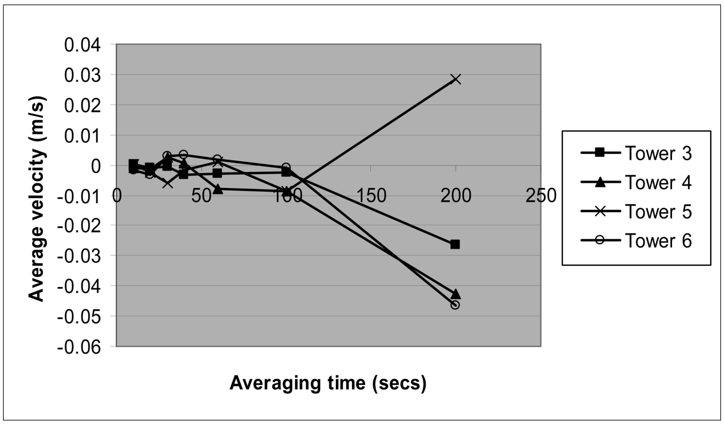

Fig. 6 Effect of moving-average time on mean value of residual turbulence

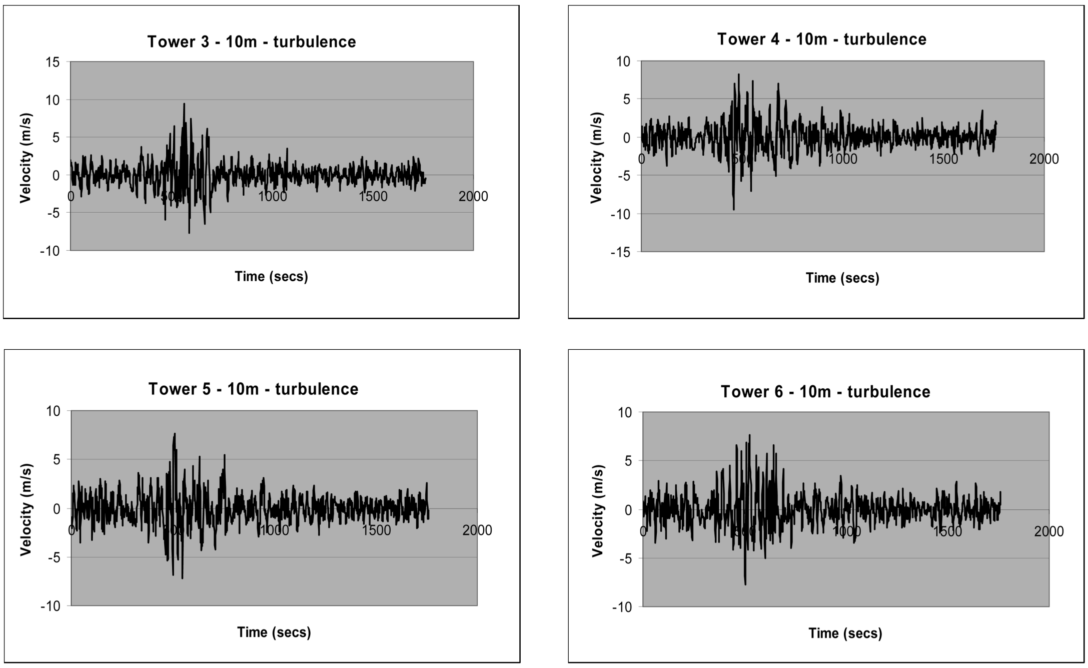

Fig. 7 Residual turbulence on four towers

are the dominant strong wind event, as such averaging times will clearly average out the features associated with the passage of the event.

On the other hand too low an averaging time, although giving a zero mean for the residual turbulence, will retain some of the random fluctuations that are not common to the other time histories. For example the top graph of Fig. 5 indicates that 10 seconds is probably too low a value in the present case. Hence, a filter with an averaging time of 40 seconds was chosen as a reasonable value of averaging time, that retains the main flow features of the event, and, when subtracted from the original time histories, results in residual turbulence with a near-zero mean value.

The 40-second running-mean time history in Fig. 5 retains some ‘oscillations’ between 700 and 1000 seconds, with a period of about 100 seconds. The origin of these features is uncertain, but may be associated with successive ring vortices on the rear side of the downdraft, as suggested by Kim and Hangan (2007). However, they are of little engineering significance as they occur when the main gust front has passed and the wind speeds are relatively low.

Fig. 7 shows the time histories of residual turbulence from Towers 3 to 6. Note that, although the mean value of the turbulence is close to zero, the data is non-stationary, with higher amplitudes at times between 500 and 600 seconds, corresponding to the times of maximum run-ning-mean wind speeds. Analysis of the statistical characteristics of the turbulence is discussed in Section 5.

4. Running mean wind speeds

As discussed in the previous section, a value of 40 seconds was selected as a reasonable value of moving averaging time that retains most of the essential flow features of the event, whilst removing the random turbulence components. The time histories obtained by filtering in this way are referred to, in this paper, as ‘running-mean’ wind speeds (following Choi and Hidayat 2002). The residual

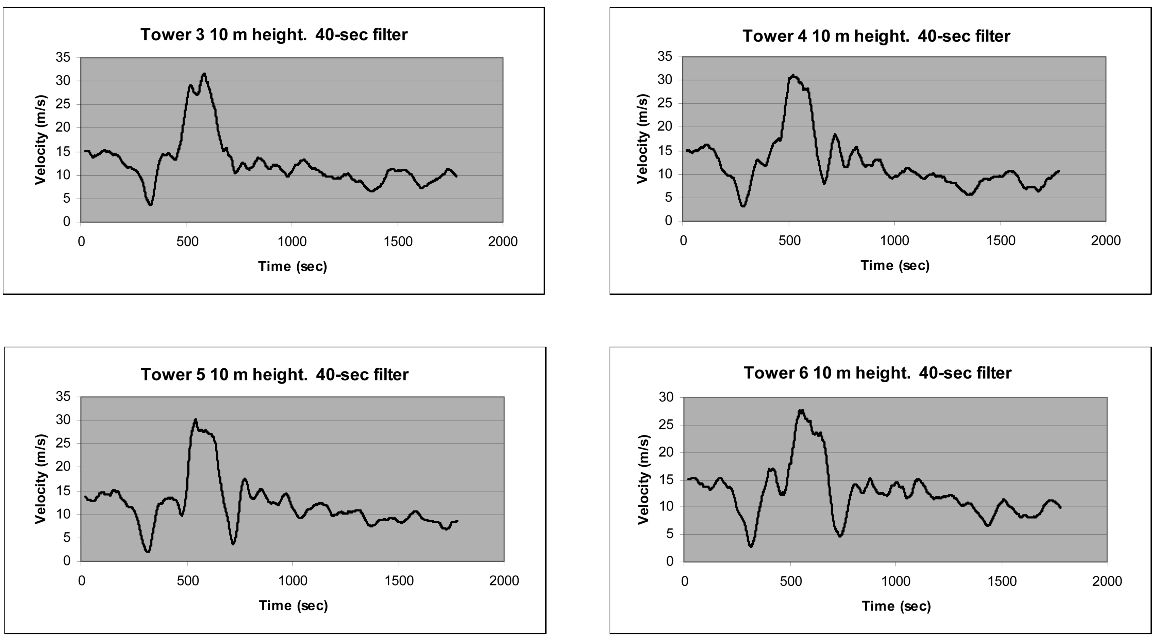

Fig. 8 Filtered ‘running-mean’ components on four different towers (40 second moving average)

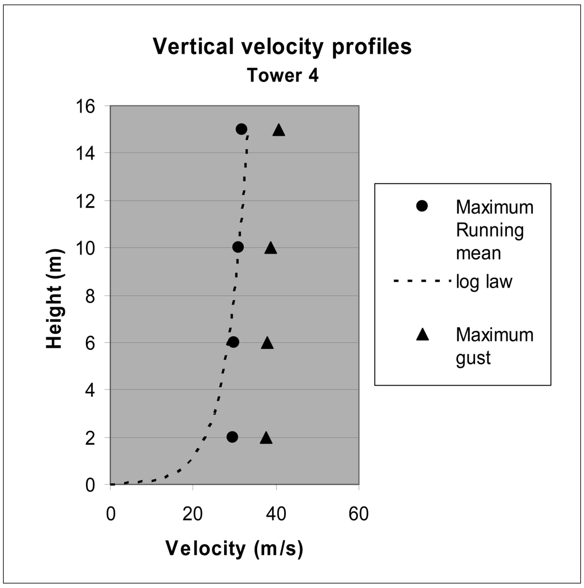

Fig. 9 Vertical profiles of maximum 'running mean' and gust speeds

turbulence is relatively small in magnitude, and hence the running mean is the dominant component.

Fig. 8 shows the filtered running-mean time histories for wind speeds at 10-metres height from Towers 3, 4, 5 and 6. Considering that the towers are spaced 263 metres apart, the time histories are remarkably similar across the four towers. This similarity has obvious consequences for the loading of structures of large horizontal extent, such as transmission lines, and it is therefore not surprising that these systems regularly fail in convective downdraft events of this type in many parts of the world (e.g. Holmes 2007, Chapter 13).

The measured vertical profiles of the maximum running-mean velocity, and of the maximum gust velocity, are shown for heights between 2 and 15 metres on Tower 4 in Fig. 9. These show only slightly increasing speed with height, and differ from boundary layer winds, as indicated by the standard logarithmic law profile (assumed roughness length for open country: 0.02 m), also shown in Fig. 9. Approximately uniform profiles for the instantaneous velocities at various time instants were also observed by Chen and Letchford (2005). Apparently, the horizontal winds in this downdraft have developed over a very short fetch length, with little retardation by friction at the ground surface. This is consistent with impinging jet flow, in which a newly formed surface layer evolves radially from the stagnation point, see Kim and Hangan (2007).

It is interesting that a similar event recorded in Brazil (reported by Ponte and Riera 2007) also indicates very little variation with height of the maximum gust over a height range of 20 to 40 metres.

5. Gust factors

A gust factor can be defined as the ratio between the largest unfiltered wind speed in the time history and the largest value of the filtered running mean wind speed. The gust factor, defined in this way, is plotted in Fig. 10 as a function of moving averaging time. The value of gust factor is fairly stable at a value of around 1.25, for averaging times between 30 and 70 seconds. This value is lower than values of 1.4 to 1.6 obtained for synoptic winds over open country, firstly because of the lower effective turbulence intensity (see Section 6.1), and secondly, because of the lower peak factors associated with the averaging times of 30 to 70 seconds. This result supports the selection of a moving average time of 40 seconds for this data, as previously discussed. The gust factor increases with increasing averaging time, but the denominator then has progressively less meaning as more and more fluctuations due to the storm passage are averaged out.

Note that the gust factor based on the 'mean' wind speed averaged over the whole record (1800 seconds) is about 3.2. This is clearly much greater than typical values obtained for synoptic boundary-layer winds for the same height and terrain – by a factor of 2 or more, and indicates the essential differences between the two wind types.

6. Turbulence characteristics

The characteristics of the residual random turbulence, obtained by subtracting the 'runningmean' wind speeds from the original time histories, are discussed in this section.

6.1. Turbulence intensity

A similar averaging, or filtering, process can be applied to the residual high-frequency turbulence components. Fig. 11 shows the root-mean-square turbulence (for Tower 4, 10 m height) calculated in a similar way to the running mean component (i.e. with a 40-second moving average calculation). The lower plot in Fig. 11 shows the 'running turbulence intensity' defined as follows:

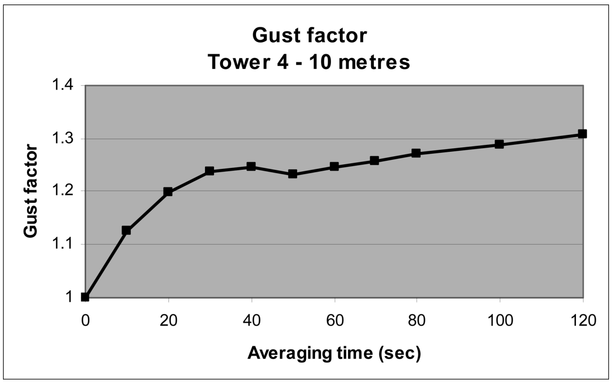

Fig. 10 Gust factor (as defined in text) as a function of moving average time

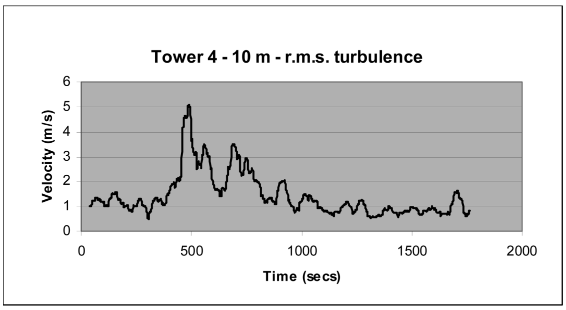

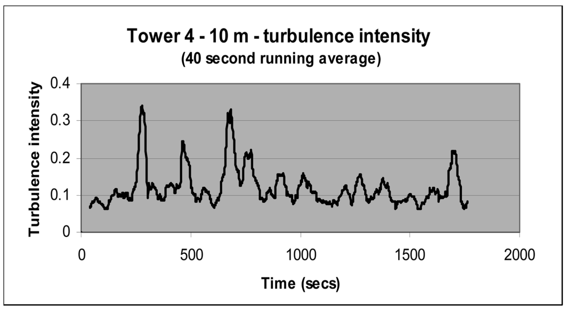

Fig. 11 r.m.s turbulence and turbulence intensities (40 second moving average)

$$I_u = \frac{\sigma_u(t)}{\tilde{U}(t)} \tag{1}$$

$\sigma_u(t)$ denotes time-varying r.m.s. turbulence (upper graph in Fig. 11) (obtained from a moving average of 40 seconds), and $\tilde{U}(t)$ denotes the running-mean wind speed. The lower graph of Fig. 11 shows the running turbulence intensity peaking at about 0.3. However, those peaks occur at about 280 seconds and 680 seconds, when the running-mean component experiences 'troughs' (Fig. 8). The more important values from a structural point of view occur at times between 500 and 600 seconds when the running mean is greater than 25 m/s. In that time range, the effective turbulence intensity is between 9 and 11%, which agrees with more sophisticated analyses and modeling by Chen and Letchford (2005). This value is lower than that in synoptic boundary-layer winds – for example, at a similar site only about 15 kilometres away, the turbulence intensity in synoptic winds at the same height of 10 metres was measured as 15-20% (Levitan and Mehta 1992). The low-frequency (i.e. with periods of 40 seconds or greater) components in the gust front are, of course, retained in the running mean component and are essentially deterministic in nature, whereas in the synoptic boundary-layer winds, they are produced by the large-scale turbulence components and are random in nature.

Gast-Orwig and Schroeder (2003, 2007) obtained larger values of turbulence intensity for this downdraft than those shown in Fig. 11. However, their averaging time of 120 seconds incorporated some of the low-frequency fluctuations that are here included in the running-mean; those fluctuations probably should be considered part of the storm characteristics, rather than random turbulence.

The effect of moving average time on the running turbulence intensity, averaged over the period during which the unfiltered wind speed is greater than 30 m/s, is shown in Fig. 12. This indicates that for averaging periods between 20 and 80 seconds, the running turbulence intensity is stable between 0.09 and 0.12, again indicating moving averaging times in this range are suitable. Lower averaging times would exclude too much of the random component from the residual turbulence; averaging times greater than 80 seconds would incorrectly *include* some of the deterministic time history resulting from the storm passage with the random turbulence.

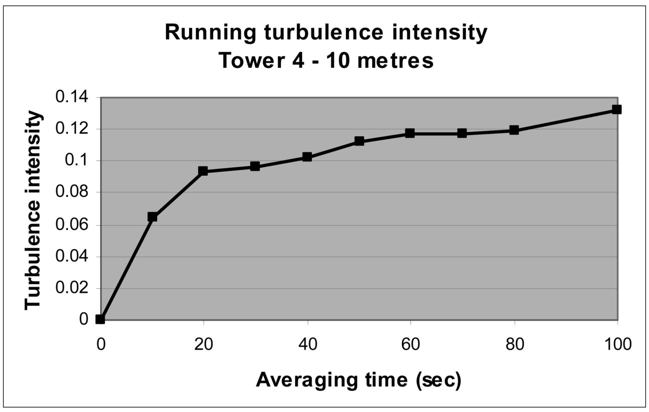

Fig. 12 Running turbulence intensity (during maximum wind period) as a function of moving average time

6.2. Spectral density and coherence

Estimates of spectral density and coherence were obtained using MATLAB software in which the time histories were divided into overlapping segments, to each of which a Fast Fourier Transforms was applied. Hanning windowing was applied to each segment. Sixteen final estimates were obtained in each case with a frequency interval of 0.03125 Hertz (the sampling interval for the time histories is 1 second).

Examples of spectral density estimates of the random turbulence, plotted against frequency, n, on log-log axes are shown in Fig. 13. The spectral density shows a decay slope only slightly greater than the -5/3 slope range (inertial sub-range) found in boundary-layer turbulence. The von Karman form of spectral density, as used in the Australian/New Zealand Standard, AS/NZS1170.2:2002 (Standards Australia 2002), (Eq. 2) is also shown in Fig. 13 as a reference line. Perhaps surprisingly, above 0.1 Hertz the measurements agree reasonably well with this form which, of course, was developed for boundary-layer winds.

$$S_u(n) = \frac{4\sigma_u L/\hat{\hat{U}}}{[1+70.8(nL/\hat{\hat{U}})^2]^{5/6}} \tag{2}$$

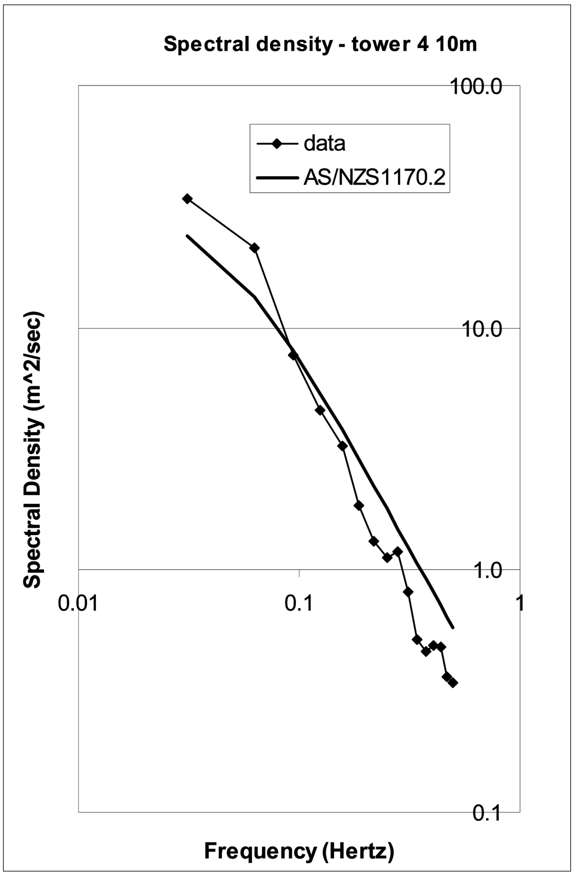

Fig. 13 Spectral densities of residual turbulence at 10m height (Tower 4)

where σ_u is the standard deviation of the turbulent wind velocity, L is the integral length scale (= 85 m at 10 m height in AS/NZS1170.2:2002), and $\hat{\tilde{U}}$ is the maximum running mean wind velocity in the record.

However, it should be noted that the low-frequency components are not included in the spectra in the present decomposition, but are treated as part of the running mean.

Root coherence for the residual high-frequency turbulence with vertical separations (from various pairs of anemometers on Tower 4, is shown in Fig. 14. The square root of coherence is plotted against the product of frequency and vertical separation distance.

A common form for root coherence used for boundary-layer turbulence in synoptic scale wind systems is:

$$\rho(n) = \exp(-k|n.\Delta z/\bar{U}|) \tag{3}$$

Using an average value of the running mean wind speed, $\bar{\tilde{U}}$, of 12 m/s, the root coherence of the turbulence for vertical separations on Tower 4 can be written as:

$$\rho(n) \cong \exp(-13.2|n.\Delta z/\bar{\tilde{U}}|) \tag{4}$$

Eq. (4) has been plotted on Fig. 14 for comparison with the measured values; reasonable agreement is obtained for the frequencies giving significant values of coherence. For atmospheric boundary layer turbulence, k is normally in the range of 5 to 15; thus the downdraft residual turbulence appears to have similar vertical coherence to atmospheric boundary-layer turbulence, with $\bar{U}$ replaced by $\bar{\tilde{U}}$. However, Chen and Letchford (2005) found that k decreased slightly with height and separation.

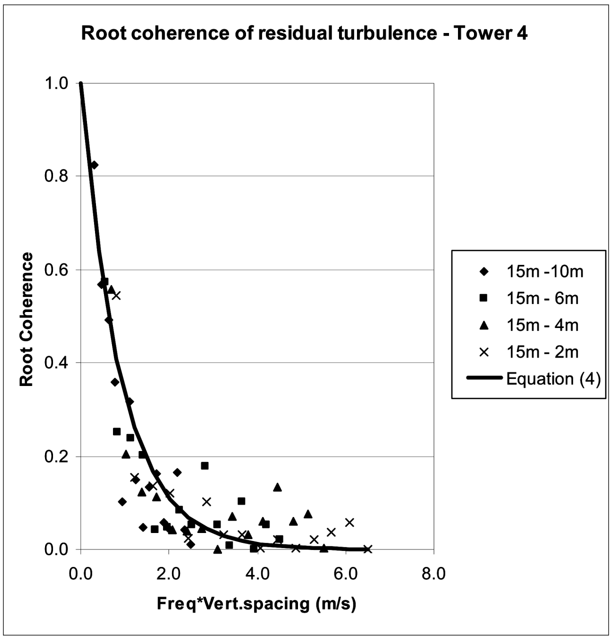

Fig. 14 Vertical coherence of residual turbulence (heights 2 to 15 m on Tower 4)

6.3. Lateral correlations and coherence

The coherences for the residual turbulence, between pairs of time histories from different towers in the array, i.e., with horizontal separations, were also determined. Samples of these are shown in Fig. 15. It is clear that the root-coherences for the turbulence from towers 263 m apart are negligible, with values between 0 and 0.15. In this range, the standard errors of root-coherence estimates are very high, and the values can be assumed to be essentially zero.

Table 1 shows correlation coefficients for the residual turbulence and 'pseudo' correlation coefficients for the 'running mean' components. 'Pseudo' indicates that the sample mean has not been subtracted when calculating the correlations – this is more appropriate for non-stationary data like this. The residual turbulence has near-zero correlations as expected from Fig. 6. As expected from Fig. 8, the running-mean coefficients have very high 'pseudo' correlation coefficients lying between 0.95 and 0.99. As the running-mean is the dominant component, this results in high 'pseudo' correlations for the total (unfiltered) wind speeds. Similar results were obtained for this

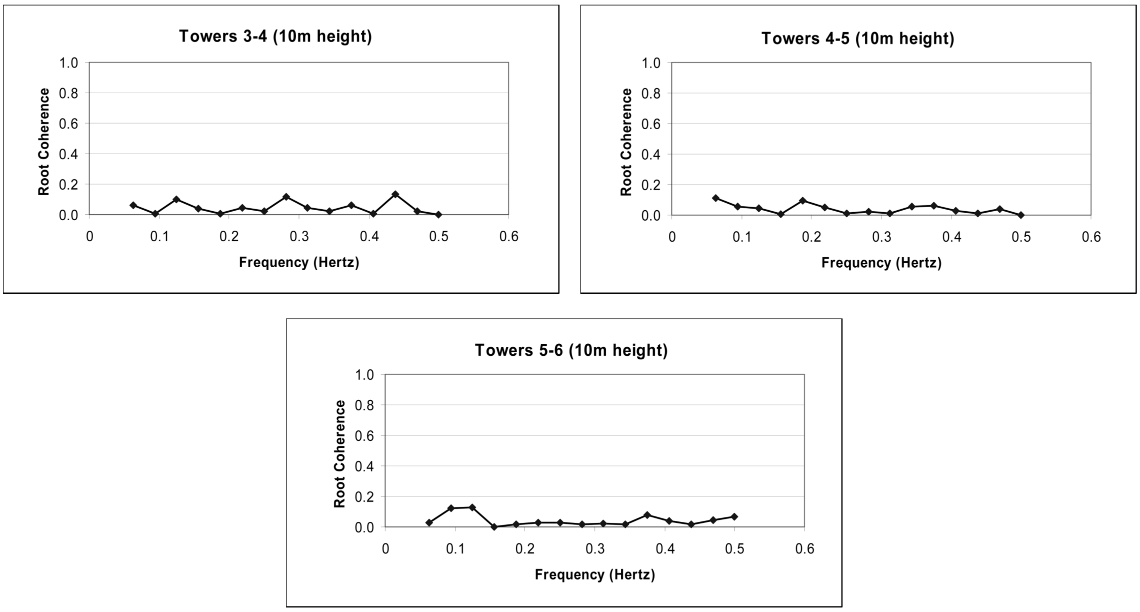

Fig 15 Lateral coherence of residual turbulence

Table 1 Correlation coefficients for horizontally-spaced anemometers (10 m height)

Pair of anemometers	Pseudo Correlation Coefficient for unfiltered data	Pseudo Correlation Coefficient for running mean	Correlation Coefficient for residual turbulence
3-4	0.963	0.979	0.044
3-5	0.967	0.981	0.100
3-6	0.966	0.982	-0.072
4-5	0.935	0.951	0.048
5-6	0.969	0.985	0.063

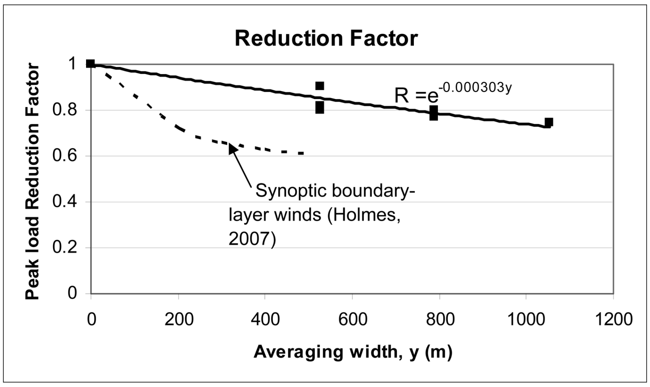

Fig. 16 Span reduction factor for peak pressures, averaged over various horizontal widths

data by Chen & Letchford (2006), using different analysis methods.

7. Span reduction factors

High voltage transmission lines typically consist of spans between support towers, or pylons, of between 400 and 500 metres. If they were impacted by the event described in this paper, they would clearly experience the full effect of the wind forces generated by the underlying running-mean wind speeds, which are very well correlated over several hundred metres, as indicated by Fig. 8 and Table 1. The residual turbulence components are, however, poorly correlated over those spans, as shown by Fig. 15 and Table 1.

To investigate the effective wind loads on systems of long horizontal extent, such as transmission lines, the time histories of wind velocity from the Lubbock-Reese downdraft, were squared, and hence became proportional to wind *pressure*, and averaged in groups of two, three or four, to simulate total wind forces over various horizontal span lengths. The reduction in peak load, as compared to that at a point, is shown as a function of transverse horizontal averaging length in Fig. 16. These ‘span reduction factors’ can be compared with those typically used for transmission line design in synoptic boundary-layer winds, which are also shown in Fig. 16 (taken from Holmes 2007, Chapter 13).

Clearly the span reduction factors in this convective downdraft wind are considerably higher than those obtained in synoptic winds, and hence the total wind load on a line, which would be required to be resisted by the tower, is considerably greater than those normally assumed in design. For example, Fig. 16 indicates a reduction factor of about 0.9 for a span of 500 metres, compared with a value of about 0.6 for synoptic winds; this corresponds to a load increase of 50%. This increase is one important reason why many transmission lines have failed in convective downdrafts in several parts of the world (e.g. Holmes 2007).

8. Conclusions

This paper has described the characteristics of the severe rear-flank downdraft that occurred near Lubbock, Texas on 4 June, 2002, from a wind engineering viewpoint. The event is significant, not just for the comprehensive set of anemometer recordings obtained at the Reese location, but also for the strength of the gust wind speeds – approximately the 50-year return period event at a point – as given by the American Standard for wind loads (ASCE 2006).

Radar images and wind speed and direction recorded at the Lubbock Airport, 22 kilometres east of Reese, indicate the event was a high-intensity large gust front, travelling towards the east at about 12 m/s. The event appears to be significantly larger than, and may differ in structure from, microbursts that have been represented as moving circular impinging jets (e.g. Fujita 1985, Kim and Hangan 2007, Holmes and Oliver 2000)

A simple moving average filter was used to decompose the time histories into dominant low-frequency deterministic components, which capture the essential flow features in the gust front, and random turbulence components. It was found that any moving average time less than about 100 seconds results in a turbulence component with a near-zero mean. A moving average time of 40 seconds was used for the present analysis, although any time between 30 and 70 seconds could reasonably have been adopted. This range of moving average times is supported by the stability of the gust factor and running turbulence intensity, as discussed in Sections 5 and 6.1 respectively.

A general conclusion of the work is that codification of wind loads based on 10-minute or hourly means is not appropriate for locations where thunderstorm downdrafts are the dominant strong wind event.

The residual turbulence components remaining after the running mean time histories are subtracted from the original time histories, appear to have similar characteristics to the high-frequency components of atmospheric turbulence in the boundary layers of synoptic winds.

In summary, the recorded wind data from the event indicates the following characteristics:

- A slowly-varying underlying ‘running-mean’ wind speed component, well correlated horizontally and vertically. This is the dominant component of the total wind speed.
- A random high frequency turbulent component, with a standard deviation of about 10% of the running mean when the velocities are highest at the peak of the event (i.e. a ‘running turbulence intensity’ of about 10%)
- The spectra of the residual turbulence components at the high-frequency end, appear to be similar to that of boundary-layer winds.
- The vertical coherence of the turbulence components is similar that of boundary-layer turbulence, when an average running-mean velocity is used for scaling.
- The effects of convective downdrafts on structural systems of large horizontal extent, such as transmission lines are discussed. In particular, it is shown that significantly higher ‘span reduction factors’ are obtained in these events, compared to those used in design, based on boundary-layer winds from large-scale synoptic systems. It is shown that 50% higher wind loads can be generated on the lines, for the same gust wind speed at a point.

Nomenclature

I_u	turbulence intensity
k	constant in exponential coherence function
L	integral length scale
n	frequency
R	span reduction factor
$S_u(n)$	spectral density of wind velocity
t	time
$U(t)$	running-mean wind velocity

$\hat{\hat{U}}$ maximum running mean wind velocity
Δz difference in heights
$\rho(n)$ root coherence
$\sigma(t)$ time-varying r.m.s. turbulence
σ_u standard deviation of wind velocity

References

American Society of Civil Engineers (2006), *Minimum Design Loads for Buildings and Other Structures*, ASCE/SEI 7-05, A.S.C.E., New York.

Chen, L. and Letchford, C.W. (2005), "Proper orthogonal decomposition of two vertical profiles of full-scale non-stationary correlated downburst wind speeds", *J. Wind Eng. Ind. Aerodyn*., **93**, 187-216.

Chen, L. and Letchford, C.W. (2006), "Multi-scale lateral correlation analyses of two lateral profiles of full-scale downburst wind speeds", *J. Wind Eng. Ind. Aerodyn*., **94**, 675-696.

Choi, E.C.C. and Hidayat, F.A. (2002), "Dynamic response of structures to thunderstorm winds", *Prog. Struct. Eng. Mech.*, **4**, 408-416.

Fujita, T.T. (1985), "Andrews AFB microburst", Dept. of Geophysical Sciences, University of Chicago, SMRP Research paper 205, December 1985.

Gast, K.D. and Schroeder, J.L. (2003), "Supercell rear-flank downdraft as sampled in the 2002 thunderstorm outflow experiment", *11th International Conference on Wind Engineering*, Lubbock, Texas, June 2-5, 2003.

Holmes, J.D. (1999), "Modeling of extreme thunderstorm winds for wind loading and risk assessment", *Proceedings, of the 10th International Conference on Wind Engineering,* Copenhagen 1999, Balkema Press, Amsterdam, 1999, pp. 1409-1455.

Holmes, J.D. (2007), *Wind loading of structures*, Taylor and Francis, U.K.

Holmes, J.D. and Oliver, S.E. (2000), "An empirical model of a downburst", *Eng. Struct*. **22**, 1167-1172.

Jeong, J. and Hussain, F. (1995), "On the identification of a vortex", *J. Fluid Mech.*, **285** 69-94.

Kim, J. and Hangan, H.M. (2007), "Numerical simulations of impinging jets with applications to down-bursts", *J. Wind Eng. Ind. Aerodyn*., **95**(4) 279-298.

Letchford, C.W., Mans, C. and Chay, M.T. (2002), "Thunderstorms – their importance in wind engineering", *J. Wind Eng. Ind. Aerodyn.*, **90**, 1415-1433.

Levitan, M.L. and Mehta, K.C. (1992), "Texas Tech Field Experiment for wind loads. Part II: Meteorological instrumentation and terrain parameters", *J. Wind Eng. Ind. Aerodyn.*, **43**, 1577-1588.

Orwig, K.D. and Schroeder, J.L. (2007), "Near-surface wind characteristics of extreme thunderstorm outflows", *J. Wind Eng. Ind. Aerodyn.*, **95**(7), 565-584.

Ponte, J. and Riera, J.D. (2007), "Wind velocity field during thunderstorms", *Wind Struct.*, **10**, 287-300.

Standards Australia, (2002). *Structural design actions. Part 2: Wind actions.* Australian/New Zealand Standard, AS/NZS 1170.2:2002.

Wakimoto, R.M. (2001), "Convectively driven high wind events", *Met. Monographs*, **29**, 255-298.

CC